17th World Conference on Earthquake Engineering, 17WCEE
Sendai, Japan - September 13th to 18th 2020

FULL-SCALE FIELD TESTS ON 1D PERIODIC BARRIERS

Y. L. Mo[(1)], H. W. Huang[(2)], J. J. Wang[(3)], F. –Y. Menq[(4)], K. H. Stokoe[(5)]

[(1)] *John and Rebecca Moores Professor, University of Houston, yilungmo@central.uh.edu (corresponding author),*
[(2)] *Ph. D. candidate, University of Houston, hhunag15@uh.edu*
[(3)] *Postdoctoral associate, University of Houston, jwang215@central.uh.edu*
[(4)] *Operations Manager, The University of Texas at Austin, fymenq@utexas.edu*
[(5)] *Jennie C. and Miltion T. Graves Chair in Engineering, The University of Texas at Austin, k.stokoe@maiWl.utexas.edu*

Abstract

The innovative seismic isolation system of periodic foundation has been proposed based on the theory of periodic metamaterial. According to the solid-state physics, the periodic metamaterials have the unique capability to manipulate the wave through the interaction between the waves and the metamaterials. Possessing the frequency-selective property, the periodic metamaterial prohibits the propagation of waves with frequencies within its frequency band gaps. Previous experimental and numerical studies have shown that a periodic foundation can significantly mitigate vibrations. However, the deployment of periodic foundation for an existing structure may be difficult. In response to this weakness, a non-invasive metamaterial-based isolation system of periodic barriers has been developed by combining the trench-type wave barrier and the 1D periodic metamaterials. The periodic barriers are designed and fabricated using reinforced concrete and synthetic rubber (polyurethane) materials. The periodic barriers can protect the structure from earthquakes and vibrations without the need to attach to the structure. Since the soil is a very complex natural material, it is necessary to do the full-scale field tests to show the practical feasibility of the periodic barrier as a seismic isolation system buried in the soil. This paper is focused on reporting full-scale field tests to validate the practical feasibility of the periodic barriers as a seismic isolation system. The test was conducted by the experimental facilities of the Natural Hazards Engineering Research Infrastructure (NHERI) at the University of Texas at Austin. Passive isolation tests were performed under various input waves, including frequency sweeping, harmonic and seismic waves. For passive isolation, a state-of-the-art shaker, T-Rex, was placed at the preselected distance from the barrier locations, and the excitations were applied in vertical, horizontal inline, and horizontal crossline modes. In this paper, the theory of periodic metamaterial is first presented. Second, the test setup, test procedure, and data processing method are illustrated. The details of the experimental results, including the originally recorded data and the evaluated vibration attenuations, are reported. The mechanism of the vibration attenuation in periodic barriers was critically examined to validate the concept of the periodic barriers.

Keywords: Periodic metamaterial; periodic barrier; full-scale field test; passive isolation; active isolation

1. Introduction

To prevent the effect caused by the earthquakes, various seismic isolation systems have been proposed and implemented. The innovative seismic isolation system of periodic material was proposed to minimize the vertical vibration and rocking of engineering structures [1-7]. The periodic material is constructed by periodically arranged unit cell with its composite materials having distinct material properties to obtain the unique characteristic of frequency band gap. The frequency band gap is the gap area in the dispersion relation of the material, where there does not exist the eigenfrequency for any wave vector along the edge of the first irreducible Brillouin zone [8]. The wave propagation will be significantly reduced when the wave possesses the frequency falling within the range of frequency band gap. By manipulating the mechanical and geometric properties of the composed materials, the desired frequency band gap can be obtained [9]. Researchers have been investigating the periodic material base seismic isolation system, periodic foundation, to reduce the response of the structure [1, 2]. It is found that significant attenuation of the response as the frequency of the dominant parts of the incident wave falls into the frequency band gap. And more reduction is achieved with increasing number of unit cells. Significant numerical and experimental study were conducted and the numerical results were validated with the experimental results [3-7].

However, for the existing structure, installation of the periodic foundation can be very difficult. Therefore, a non-invasive seismic isolation method based on the periodic material, the periodic barrier, becomes an alternative. The periodic barrier is the periodic material based wave barrier that can be built around the structure. The idea of wave barriers originates from preventing the man-made vibration from disturbing and damaging the surrounding structures by creating a discontinuity in the path of wave propagation. The open and infilled trenches are the typical forms of conventional wave barriers. With the help of the wave barrier, the reduction of the response can be achieved. Based on the framework of the conventional wave barriers, the periodic materials are proposed as innovative infilled materials for the barrier [10-13]. This type of barrier is called periodic barrier in this study. To extend the application of periodic material to the underground structures and to build a non-invasive seismic isolation system around the protected structures, the periodic barrier is developed in this study. The periodic barrier is the underground seismic isolation system built around the protected structure against the disturbance from seismic waves [14-16]. Since the periodic barrier is not directly attached to the structure, the installation of the periodic barrier does not affect the function of the protected structure. By using the periodic material as the infilled material, the incoming wave within the frequency band gap of the periodic barrier can be mitigated. Therefore, the periodic material can be properly designed to attenuate the waves that have the main frequencies falls into its frequency band gap. The proposed periodic barrier is made of one dimensional (1D) layered periodic barrier, which means the unit cells of the periodic material are periodic layered in one direction. This layered periodic material is the simplest form of the periodic material. Even though the numerical studies had shown the screening effectiveness of the periodic barrier, the experiment has rarely been done before. For the 1D layered periodic barrier subjected to excitation within 15 to 100 HZ, there is a dearth of large scale experimental data.

This study reports a preliminary experimental program to investigate the screening performance of the periodic barrier. The field test was conducted at the large field site managed by Hornsby Bend Biosolids Management Plant (HBBMP) located southeast of Austin. The top soil layer of the site consists mostly of sandy clay. The attenuation of motion on the surface is critical for testing the screening effectiveness of the periodic barrier. The hydraulic mobile shaker operated by NHERI@UTexas was used to apply the excitation on the ground surface.

2. Theoretical study

The dispersion relation of the periodic material provides the information of the band gap of the designed periodic material. The dispersion relation of the periodic material can be obtained from solving the wave equations with the existence of the periodic boundary condition [17].

Layered periodic material is the simplest form of periodic material. The layered periodic material has the unit cells stacked in one direction, and each of the unit cell is composed of two or more distinct materials. Figure 1 illustrates a layered periodic material with 3-layered unit cell.

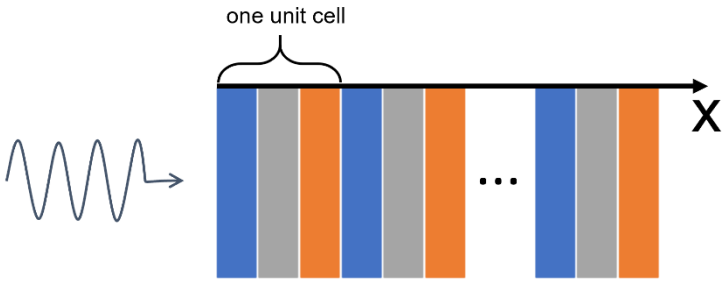

Figure 1 - Schematic of the 1D layered periodic barrier

Assume the unit cell of the layered periodic material composes of N layers of distinct material, and each layer in a unit cell is assumed to be homogenous, isotropic and satisfy the wave equation. In this study, the excitation is applied perpendicular to the propagation direction, the energy is expected to carry mostly in the form of shear wave (S wave) with larger amplitude on the surface. Using the transfer matrix method, the dispersion relation of the periodic material subjecting the S wave can be obtained. The derivation starts from solving the wave equation for homogenous materials of S wave in each layer n within a unit cell.

$$\frac{\partial^2 u_n}{\partial t^2} = C_S^2 \frac{\partial^2 u_n}{\partial x_n^2} \tag{1}$$

where C_s denotes the S wave speed of the material.

$$C_S = \sqrt{\mu_n / \rho_n} \tag{2}$$

Consider a steady state oscillatory waves of angular frequency

$$u_n(x_n, t) = \mathrm{e}^{i\omega t} u_n(x_n) \tag{3}$$

Substituting Eq. (3) into Eq. (1)

$$C_S^2 \frac{\partial^2 u_n(x_n)}{\partial x_n^2} + \omega^2 u_n(x_n) = 0 \tag{4}$$

The displacement and stress components can be expressed as

$$\begin{bmatrix} u_n(x_n) \\ \tau_n(x_n) \end{bmatrix} = \begin{bmatrix} \sin(k_S x_n) & \cos(k_S x_n) \\ \mu k_S \cos(k_S x_n) & -\mu k_S \sin(k_S x_n) \end{bmatrix} \begin{bmatrix} A_n \\ B_n \end{bmatrix} \tag{5}$$

$$\mathbf{w}_n(x_n) = \mathbf{H}_n(x_n)\boldsymbol{\psi}_n \tag{6}$$

where k_S denotes the wave number, μ_n is the Lame constant, and ρ_n is the density.

$$k_S = \omega / C_S \tag{7}$$

The thickness of the layer n is denoted as h_n. The displacement and stress of entering face $\mathbf{w}_n^L = \mathbf{w}_n(0)$ and exiting face $\mathbf{w}_n^R = \mathbf{w}_n(h_n)$ of the layer n are related through a transfer matrix $\mathbf{T_n}$.

$$\boldsymbol{w}_n^R = \boldsymbol{T}_n \boldsymbol{w}_n^L = \boldsymbol{H}_n(h_n)\boldsymbol{H}_n^{-1}(0)\boldsymbol{w}_n^L \tag{8}$$

The entering face of the 1st layer and the exiting face of the last N^{th} layer can be related.

$$\mathbf{w}_N^R = \prod_{i=N}^{1}\left[\mathbf{H}_i\left(h_i\right)\mathbf{H}_i^{-1}\left(0\right)\right]\mathbf{w}_1^L = \mathbf{T}\left(\omega\right)\mathbf{w}_1^L \tag{9}$$

Based on the Bloch theorem[18], the periodic boundary conditions can be expressed as

$$\mathbf{w}_N^R = e^{ika}\mathbf{w}_1^L \tag{10}$$

Where k is the wave number and a is the thickness of the unit cell.

The dispersion relation of the periodic material can be obtained by solving the eigenvalue problem

$$\left|\mathbf{T}(\omega) - \mathrm{e}^{ika}\mathbf{I}\right| = 0 \tag{11}$$

The dispersion relation of the periodic material provides information about the frequency band gap.

3. Experimental program

3.1. Specimen description

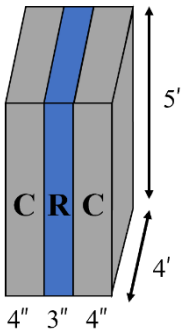

Figure 2 – Unit cell

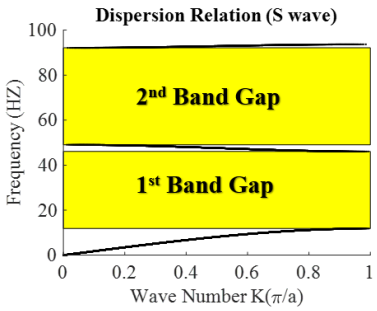

Figure 3 - Dispersion relation of the unit cell in Figure 2.

To build the periodic barrier as the countermeasure against the earthquake, the periodic barrier in this study is made of the common materials used in civil engineering practice. The designed periodic barrier has height of 5 ft (1.5 m) and length of 4 ft (1.2 m) as illustrated in Figure 2. The unit cell of the periodic barrier consists of 2 concrete layers and 1 rubber layer with the thickness of 4 in (0.1016 m) and 3 in (0.0762 m) respectively. The concrete layer and rubber layer are denoted as C and R respectively in Figure 2. The mechanical properties are presented in Table 1.

Table 1. Mechanical and geometric properties of the composed materials

Material	ρ (kg/m^3)	E (GPa)	υ	h (m)
Concrete	2400	30.44	0.2	0.1016
rubber	1100	0.0001586	0.463	0.0762

By solving the eigenvalue problem with the given material and geometric properties of the unit cell, the resulting dispersion relation of the periodic barrier subjected to S wave is shown in Figure 3, which provides the information of the frequency band gap. The first three frequency band gaps are 11.82-46.06, and 49.06-92.12 HZ when the periodic barrier is subjected to S waves.

3.2. Test setup

The tests were carried out using the tri-axial shaker, T-Rex, operated by NHERI@UTexas. The attenuation of motion on the surface is critical for investigating the vibration mitigation performance of the periodic barrier. T-Rex is ideal for testing the performance of the periodic barrier, since the excitation generated by the shaker has the higher energy near the ground surface, and this type of excitation is difficult to accomplish on a shake table or in a centrifuge model. The experiment was divided into two stages: w/ and w/o the periodic barrier. For each stage, the shaker was placed at the preselected distance of 6.1 m and 24.4 m away from the barrier face, and a series of fix-frequency continuous sine wave was conducted. In the fix-frequency continuous sine wave test, the shaker generated continuous vibrations with fixed frequencies within the duration of 2 sec. The exciting frequencies ranging from 15 to 100 HZ with an interval of 5 HZ were used.

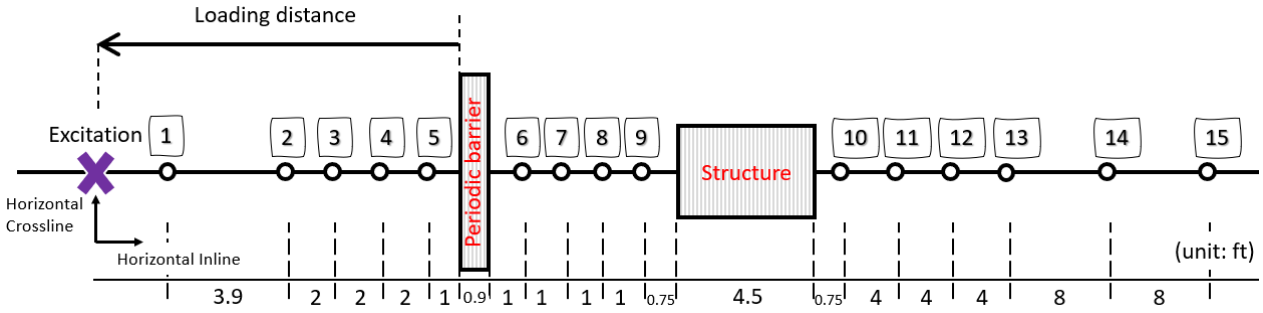

Figure 4 - Plan view of the field test layout (in units of ft)

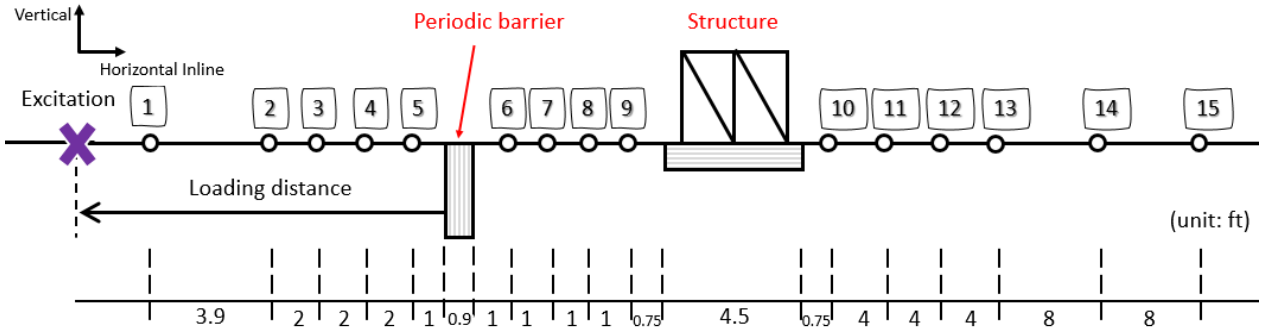

Figure 5 - Side view of the field test layout (in units of ft)

The layout of sensors, structure, periodic barrier and the loading point is illustrated in Figure 4 and Figure 5. A geophone is a device that converts ground movement (velocity) into voltage, which may be recorded at a recording station. A total of 45 geophones were placed for 15 preselected locations before and after the periodic barrier to measure the ground velocity of the ground surface during the excitation. For each location, three geophones were installed at each location to measure the response in vertical, horizontal crossline and horizontal inline directions. The sensors were placed based on the measuring distance for evaluating the performance of periodic barrier. The measuring distance is set to be one time of Rayleigh wave wavelength. With the assumed soil properties: Young's modulus of 20 MPa, density of 200 kg/m^3, and Poisson ratio of 0.25, the corresponding Rayleigh wavelength varies from 40 ft (12.2 m) to 6 ft (1.8 m) for the frequency ranging from 15 HZ to 100 HZ. The arrangement of the geophones can cover all possible Rayleigh wave wavelengths from behind the periodic barrier and there were at least 4 sensors in each direction within the shortest Rayleigh wavelength, 6 ft, from the face of the barrier.

Figure 6 - Field test setup

The test setup started with marking the positions of the structure, sensors, and shaker. After the preselected positions were marked, the shaker was moved to the designated position, and geophones were installed for all three directions at each location. In order to get accurate results, the geophones were leveled using the bubble level. The geophone has its natural frequency of 4.5 HZ. The geophone collects the response in the rate of 2048 HZ.

3.3. Loading protocol

The fix-frequency continuous sine waves generated from the shaker were applied on the surface in horizontal crossline direction at two preselected positions, 6.1 m and 24.4 m from the face of periodic barrier. The responses were recorded by the geophones at all 15 locations within the duration of the excitation. Prior to the installation of periodic barrier, the first stage of tests was conducted on soil without periodic barrier to serve as a reference test. The measurement results from the first stage of tests served as the reference to evaluate the performance of the periodic barrier. The second stage of the tests was conducted when there exists the periodic barrier. The test began with excavation of a rectangular trench with the width of 11 inches (0.3 m), depth of 5 ft (1.5 m), and length of 4 ft (1.2 m). After the trench was made, the prefabricated periodic barrier was put into the trench to fill the trench. The steel structure was placed for both stages for the purpose of testing the active isolation, which will be conducted in the future.

4. Experimental result

4.1. Data processing

Before analyzing the data, the Tukey window, which is a cosine-tapered window, with the cosine fraction of 0.12 was used to make the signal outside the recording duration be zero. After the windowing the signal, a 5th order low-pass, high-pass Butterworth filter, which is an anti-aliasing filter, were applied to the recording. To eliminate the response at natural frequency of the geophones, since the natural frequency of the geophone is 4.5 HZ, the low-pass cut off frequency is set to be 5 HZ, so the signal below 5 HZ can be attenuated. The signal captured by geophones were calibrated with the calibration factor of 58.4962 V/(mm/sec), and the data were converted to velocity. The data was later converted from velocity to acceleration by taking the forward difference of the velocity reading.

4.2. Frequency response function (FRF)

The screening effectiveness of the periodic barrier is defined by frequency response function, *FRF*, which is calculated from average reduction factor (*RF*). Figure 7 presents how the experimental data was interpreted for the screening effectiveness of the periodic barrier.

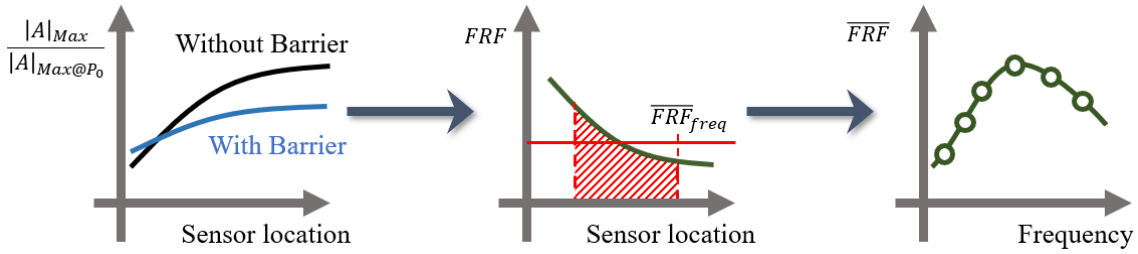

Figure 7 - Data interpretation

When the loading is a fix-frequency continuous sine wave, it was found that the signal will have the spikes before it reaches a steady response. After excluding those spikes, the maximum steady state response can be extracted at each recording point for every exciting frequency. The data is interpreted following the schematic plot in Figure 6. *RF* is a typical measure to evaluate the effectiveness of the wave barrier by comparing the normalized response of the soil surface in the presence of the wave barrier (R_w) with the response without the wave barrier (R_{wo}).

$$RF = \frac{R_w}{R_{wo}} \tag{12}$$

The normalized response at each recording point is calculated by dividing the maximum response with the maximum response at a point right before the barrier (P_0).

$$R_w = \frac{|A_w|_{\max}}{|A_w|_{\max@P_0}} \tag{13}$$

$$R_{wo} = \frac{|A_{wo}|_{\max}}{|A_{wo}|_{\max@P_0}} \tag{14}$$

where $|A_w|$ is the absolute value of acceleration record when there is barrier and $|A_{wo}|$ is the absolute value of acceleration record when there is no barrier.

In this research, the vibration isolation performance of periodic barrier was evaluated in terms of the average reduction factor $\overline{RF}$, which is a average of the normalized response over a certain distance from the face of the periodic barrier. The smaller average reduction factor indicates that the barrier is more effective. The average amplitude reduction factor is calculated as follows:

$$\overline{RF} = \frac{1}{L}\int_0^L RF \; dx \tag{15}$$

In this study, L is selected to be 1 times Rayleigh wave wavelength λ_R.

Calculated by comparing the normalized responses between the stages w/ and w/o the periodic barrier at each recording point, FRF is a typical way to quantify the screening effectiveness of the periodic barrier.

$$FRF = 20\log\left(\overline{RF}\right) \tag{16}$$

where negative *FRF* shows a reduced response, while positive *FRF* shows an amplified response.

Taking the average over the distance of 1 λ_R from the edge of the periodic barrier, the average FRF under each exciting frequency can be evaluated.

4.3. Maximum normalized response under the fix-frequency sine wave excitation

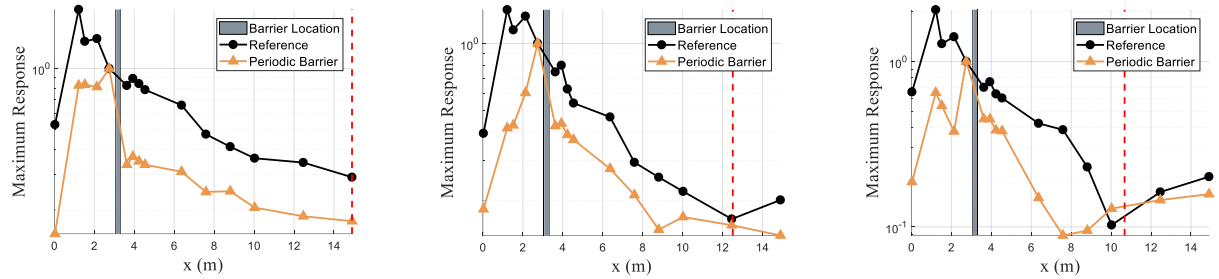

(a) 15 HZ (b) 20 HZ (c) 25 HZ

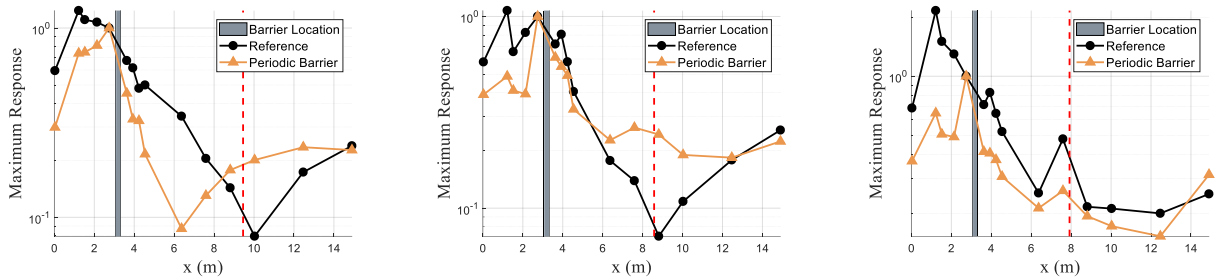

(d) 30 HZ (e) 35 HZ (f) 40 HZ

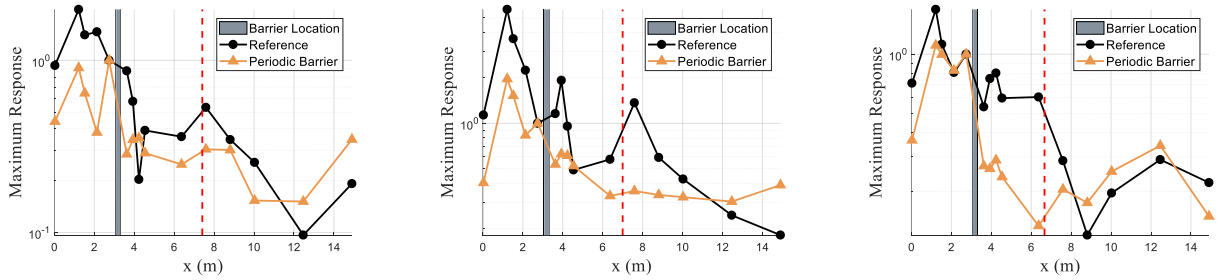

(g) 45 HZ (h) 50 HZ (i) 55 HZ

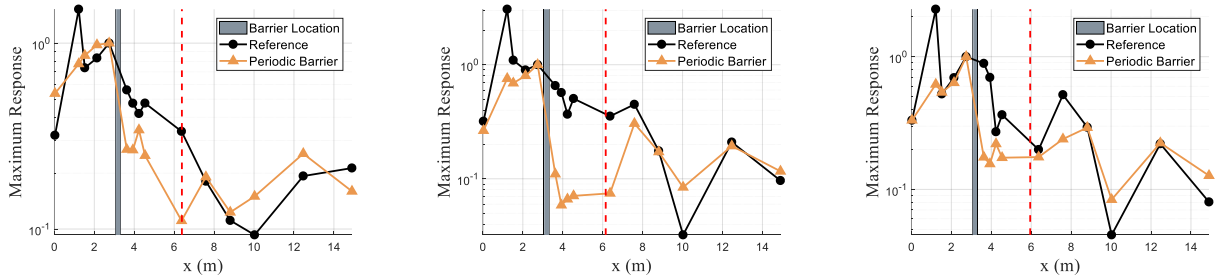

(j) 60 HZ (k) 65 HZ (l) 70 HZ

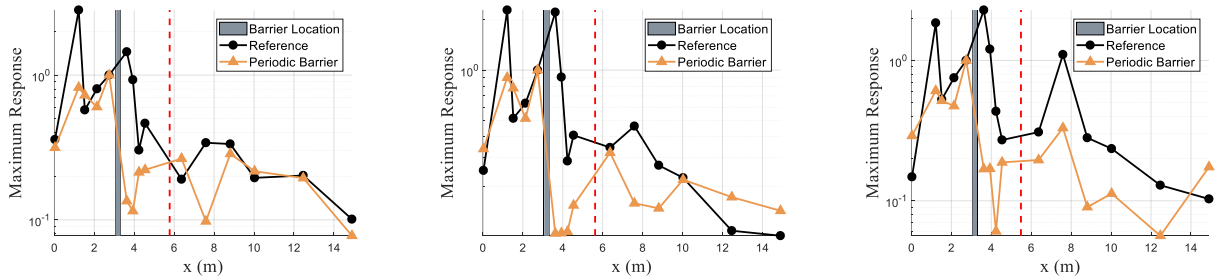

(m) 75 HZ (n) 80 HZ (o) 85 HZ

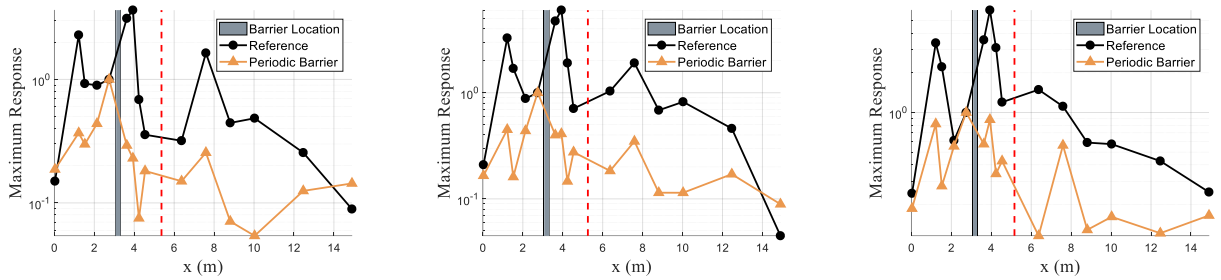

(p) 90 HZ (q) 95 HZ (r) 100 HZ

Figure 8 - Normalized horizontal crossline response under horizontal crossline excitation at 6.1 m from periodic barrier

Even though the field tests were conducted for both loading distance of 6.1 m and 24.4 m, Figure 8 only reveals the results for the loading distance equals to 6.1 m. Figure 8 shows the maximum normalized response at each sensor location under the continuous harmonic excitation applied at 6.1 m away from the barrier in horizontal crossline direction. The x-axis is the location measured from the location of the sensor labeled number 1 in Figure 4. The y-axis is the maximum response in log scale. The grey rectangular region represents the designate location of the periodic barrier. The farther sensors are less significant to the screening performance of the periodic barrier, as the depth to Rayleigh wavelength ratio is smaller when the frequency is higher. Therefore, λ_R, which is dependent on the exciting frequency, is chosen to be the measuring distance. The red dotted line indicates the measuring extent for evaluating the screening performance of the periodic barrier.

Two sets of test data are presented in each subplot that the black circle shows the normalized horizontal crossline response for the stage without the barrier, and the orange triangle is the normalized horizontal crossline response for the stage when the periodic barrier was installed, which are denoted as Reference and Periodic barrier respectively in the legend. Since the normalized response is defined by dividing the maximum steady-state response with maximum steady-state response of the point before the wave enters the periodic barrier, it can be seen in Figure 8 that the normalized response of the point before the barrier is always 1.

Geometric decay is generally seen as the sensor gets farther away from the loading point. However, the characteristics of the testing site, such as boundary or soil constituents, can have a great influence on the resulting ground response. Shown in Figure 8, some sensors were found to have a larger response than the sensors closer to the loading point. This phenomenon is attributed to the site characteristics. Since the testing site is not made of homogenous soil type and has the layers and boundaries, the resonance and reflections can result in responses that don't decay as expected in the homogenous, infinite boundary site. By comparing the response at the same point from the same site, the effect of site characteristics can be eliminated.

Figure 8 (a-r) shows that for each input vibration frequency, the notable reduction was observed for most of the sensors arranged behind the periodic barrier except for the case when 35 HZ excitation was applied. This comparison showed that the periodic barrier had notable vibration isolation performance under the horizontal crossline wave. When comparing the response of the two stages, the reduction was observed for the sensor adjacent to the periodic barrier for all exciting frequency in varying degrees. As the sensors locate farther from the periodic barrier, the response can be either reduced or amplified based on different exciting frequencies. This result may be attributed to the limited dimension of the periodic barrier in the test, which caused some vibration to be transferred from the side of the periodic barrier.

4.4. Screening effectiveness of the periodic barrier

When the loading in the horizontal crossline direction was applied, the response in the horizontal crossline direction was analyzed. The response reduction caused by the periodic barrier was obtained by comparing the ground motion w/ and w/o the periodic barrier when fix-frequency continuous sine wave load is applied. For each exciting frequency, the resulting FRF was obtained by averaging the FRF of all the sensors within the measuring distance from the face of the periodic barrier. The attenuation zone is identified as the FRF is negative. As shown in Figure 9, the attenuation zone is found within the theoretical frequency band gap, which

is highlighted in yellow. When the loading distance is 6.1 m, the reduction can be found almost for all exciting frequencies ranging from 15 HZ to 100 HZ. When the loading distance is 24.4 m, some amplifications were observed for exciting frequency within the passband. The amplifications and reductions for the loading distance of 24.4 m are more distinct compared to the loading distance of 6.1 m. It shows that the loading distance can have a significant influence on the response reduction. It can be explained by the dimension limitation. When the loading distance is longer, the ratio of barrier length to the loading distance is smaller, so the response is attributed less from the periodic barrier.

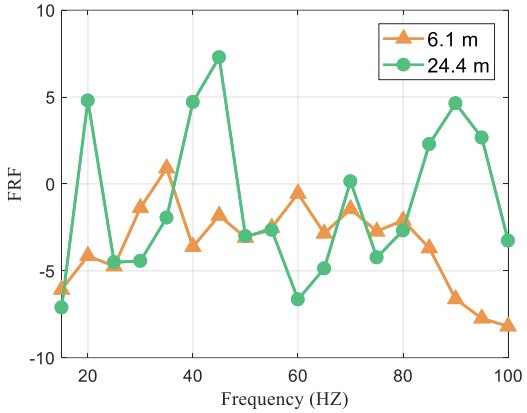

Figure 9 - Performance of the periodic barrier subjected to horizontal crossline excitation

5. Conclusion

The fix-frequency continuous sine wave tests were conducted with two loading distances. The exciting frequencies ranging from 15 to 100 HZ with 5 HZ interval were used. It is found that under the excitation in the horizontal crossline direction, significant attenuation can be seen within the theoretical frequency band gap of the designed periodic barrier.

(1) Periodic barrier can significantly affect the ground response. From Figure 8, the attenuation is observed at the measuring points right behind the periodic barrier for all exciting frequencies.

(2) The exciting frequency can result in different levels of response reduction or amplification. The attenuation zone of 25-35 HZ and 60-80 HZ can be clearly identified from the experimental results. This range of frequencies falls right in the frequency band gap. The maximum reduction is found when the exciting frequency is 65 HZ for both loading distance of 6.1 m and 24 m.

(3) The loading distance has a significant influence on the performance of the periodic barrier. When the loading distance is shorter, the attenuation and amplification are more significant. Due to the dimension limitation, when the loading distance is longer, which means the barrier length to loading distance ratio is small, the response is contributed less by the barrier, so the response is attributed less from the periodic barrier, and more from the site characteristics such as the boundary, layers and soil properties.

6. Acknowledgment

The project is sponsored by National Science Foundation under grant 1761659.

7. Copyrights

8. References

[1] Bao J, Shi ZF, Xiang HJ (2011): Dynamic responses of a structure with periodic foundations. *Journal of Engineering Mechanics, 138*(7), 761-769.

[2] Bloch F (1929): Über die quantenmechanik der elektronen in kristallgittern. *Zeitschrift für physik, 52*(7-8), 555-600.

[3] Brillouin L (1953): Wave propagation in periodic structures: electric filters and crystal lattices.

[4] Brûlé S, Javelaud EH, Enoch S, Guenneau S (2014): Experiments on seismic metamaterials: molding surface waves. *Physical review letters, 112*(13), 133901.

[5] Cheng ZB, Shi ZF (2018): Composite periodic foundation and its application for seismic isolation. *Earthquake Engineering & Structural Dynamics, 47*(4), 925-944.

[6] Dertimanis VK, Antoniadis IA, Chatzi EN (2016): Feasibility analysis on the attenuation of strong ground motions using finite periodic lattices of mass-in-mass barriers. *Journal of Engineering Mechanics, 142*(9), 04016060.

[7] Huang JK, Shi ZF (2011): Application of periodic theory to rows of piles for horizontal vibration attenuation. *International Journal of Geomechanics, 13*(2), 132-142.

[8] Huang JK, Shi ZF (2013): Attenuation zones of periodic pile barriers and its application in vibration reduction for plane waves. *Journal of sound and vibration, 332*(19), 4423-4439.

[9] Krödel S, Thomé N, Daraio C (2015): Wide band-gap seismic metastructures. *Extreme Mechanics Letters, 4*, 111-117.

[10] Palermo A, Krödel S, Marzani A, Daraio C (2016): Engineered metabarrier as shield from seismic surface waves. *Scientific reports, 6*, 39356.

[11] Palermo A, Vitali M, Marzani A (2018): Metabarriers with multi-mass locally resonating units for broad band Rayleigh waves attenuation. *Soil Dynamics and Earthquake Engineering, 113*, 265-277.

[12] Witarto W, Nakshatrala, KB, Mo, Y-L (2019): Global sensitivity analysis of frequency band gaps in one-dimensional phononic crystals. *Mechanics of Materials*.

[13] Witarto W, Wang SJ, Nie X, Mo YL, Shi ZF, Tang Y, Kassawara RP (2016): Analysis and design of one dimensional periodic foundations for seismic base isolation of structures. *International Journal of Engineering Research and Applications, 6*(1), 5-15.

[14] Witarto W, Wang SJ, Yang CY, Nie X, Mo YL, Chang KC, Tang Y, Kassawara RP (2018): Seismic isolation of small modular reactors using metamaterials. *AIP Advances, 8*(4), 045307.

[15] Witarto W, Wang SJ, Yang CY, Wang JJ, Mo YL, Chang KC, Tang Y (2019): Three-dimensional periodic materials as seismic base isolator for nuclear infrastructure. *AIP Advances, 9*(4), 045014.

[16] Yan Y, Cheng Z, Menq FY, Mo YL, Tang Y, Shi ZF (2015): Three dimensional periodic foundations for base seismic isolation. *Smart Materials and Structures, 24*(7), 075006.

[17] Yan Y, Laskar A, Cheng Z, Menq FY, Tang Y, Mo YL, Shi ZF (2014): Seismic isolation of two dimensional periodic foundations. *Journal of Applied Physics, 116*(4), 044908.

[18] Yeh P, Yariv A, Hong C-S (1977): Electromagnetic propagation in periodic stratified media. I. General theory. *JOSA, 67*(4), 423-438.

